

LIBRARY Michigan State University

This is to certify that the

thesis entitled

The Ultrastructural Development of Sporangiospores in Multispored Sporangia of Zygorhynchus heterogamus

presented by

Richard Edward Edelmann

has been accepted towards fulfillment of the requirements for

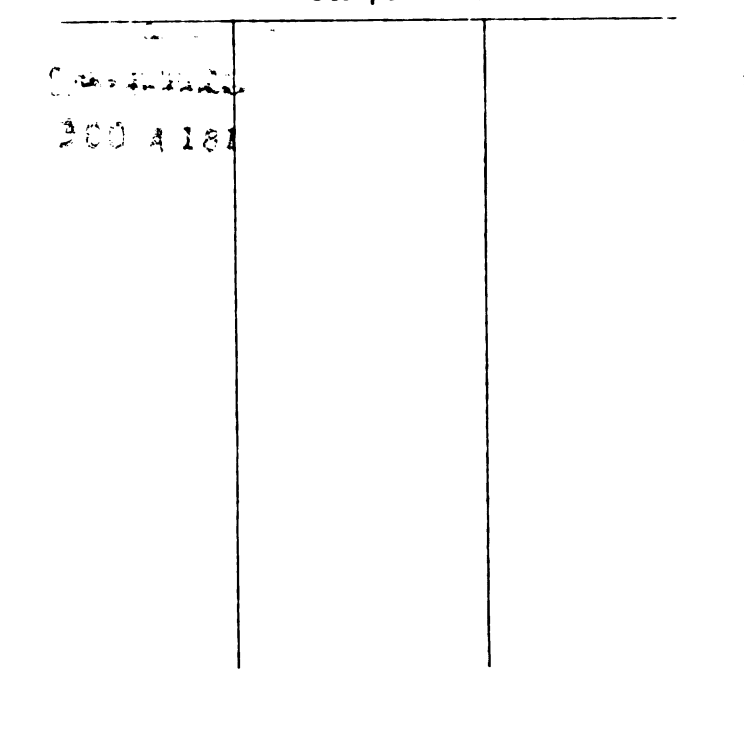
M.S. degree in Botany

Date August 12, 1988

HHES W



RETURNING MATERIALS:
Place in book drop to remove this checkout from your record. FINES will be charged if book is returned after the date stamped below.



THE ULTRASTRUCTURAL DEVELOPMENT OF SPORANGIOSPORES IN MULTISPORED SPORANGIA OF ZYGORHYNCHUS HETEROGAMUS

Ву

Richard Edward Edelmann

A THESIS

Submitted to
Michigan State University
in partial fulfillment of the requirements
for the degree of

MASTER OF SCIENCE

Department of Botany and Plant Pathology
1988

ABSTRACT

THE ULTRASTRUCTURAL DEVELOPMENT OF SPORANGIOSPORES IN MULTISPORED SPORANGIA OF ZYGORHYNCHUS HETEROGAMUS

Bv

Richard Edward Edelmann

The ultrastructural development of multispored sporangia in Zygorhynchus heterogamus Vuil. was studied, utilizing both transmission and scanning electron microscopy, and was found similar to the established general model of multispored Shortly after the initiation of sporangiosporogenesis. sporangial swelling numerous cleavage vesicles appeared within the highly vacuolate sporangium. These vesicles fused and ramified throughout the sporangium and formed an interconnected network of cleavage furrows, lined with electron opaque granules, which isolated the multiorganelled cytoplasm of the spore protoplasts. Synchronous with spore cleavage, the electron opaque granules fused and formed the exterior spore wall layer. As the spore cytoplasm condensed, the spore walls matured with a corresponding reduction of electron translucent material between the spores. With autolysis of the columellar cytoplasm, numerous vesicles appeared within the columella and fused with its plasma membrane. At the same time degradation of the sporangial wall occurred, followed by the release of mature spores.

To my parents for their love and support.

To Anne L. Gohlke for life beyond the silver rainbow.

ACKNOWLEDGEMENTS

I wish to thank Dr. Karen L. Klomparens for her expertise, help and patience as I constantly proposed new ideas for the ultrastructural development of Zygorhynchus heterogamus, as well as several other fungi, as well as editing this thesis, and training me in the use of the JEOL 100CX II. Dr. Terrence M. Hammill originally suggested the idea that the columella released the sporangial wall degradative enzymes into the sporangial matrix 1983 over lunch, as well as introducing me to the joys of fungal ultrastructure. I wish to thank Drs. Everett S. Beneke and Avlin L. Rogers for the original culture of Zygorhynchus heterogamus. I wish to thank Dr. Gary Mills for his help with the physiology of spore wall synthesis. I also wish to acknowledge Dr. Stanley L. Flegler for his assistance with the use of the JEOL 35C and JEOL 35CF, and Dr. John Heckman for his photographic technical assistance with my pestering questions.

TABLE OF CONTENTS

List of figures vi Abbreviations xi
Introduction 1
Materials and Methods 9
Cultures 9
Scanning Electron Microscopy 10
Transmission Electron Microscopy
X-ray Analysis
Light Microscopy 14
Results
Precleavage 15
Cleavage 22
Postcleavage 28
Additional Observations 41
Discussion45
List of references 53

LIST OF FIGURES

Figures Pa	age
1. Diagram (reprinted from Hammill, 1981) summarizing the process of sporangiospore formation	3
 Cutaway three-dimensional interpretive drawing (reprinted from Bracker, 1968) showing the author's concept of the cleavage apparatus during early cleavage (I), mid-cleavage (II), and late cleavage (III)	6
3. Rupture of the sporangiophore through the agar substrate	16
4. Aerial sporangiophore elongation	16
5. Straight, unbranched sporangiophore elongation prior to sporangial swelling	16
6. Initiation of sporangial swelling	16
7. Sporangial swelling and initiation of spine formation during mid-precleavage	17
8. Late precleavage sporangial swelling and spine elongation with and absence of spines near the sporangial base	17
 Sporangium with a central vacuolate region (VR), and a denser periphery 	19
10. The sporangial cytoplasm shows nuclei (N) closely associated with an interconnecting network of endoplasmic reticula (ER), mitochondria (Mt), and lipids (L)	19
11. The denser sporangial peripheral cytoplasm contains numerous cleavage vesicles (CV) containing electron opaque granules, along with nuclei (N) closely associated with ER, mitochondria (Mt), and lipids (L)	20

12.	Mid-precleavage cleavage vesicles (CV), which contained an electron opaque granular matrix, exhibited the characteristic alignment of electron opaque granules along their periphery (indicated by the arrow heads) just inside the cleavage vesicle plasma membrane. At this stage the initiation of the fusion of the these granules began	20
13.	The central vacuolate region exhibits typical mitochondria (Mt) as well as degenerate mitochondria (DM), and vacuoles containing crystalline granules (Vg)	20
14.	At this stage the sporangial matrix appears uniformly vacuolate, note nuclei (N)	21
15.	The sporangial matrix shows a general distribution of cleavage vesicles (CV)	21
16.	Early cleavage sporangium with elongated spines	23
17.	Late precleavage sporangium with shorter spines, spineless sporangial base (double ended arrow), and smooth transition (arrows) from sporangiophore to sporangium	23
18.	Early cleavage sporangium with a right angle transition from sporangiophore and sporangium (arrow)	23
19.	Late cleavage sporangium with grooved ring (arrows) indicating the presence of an internal columella	23
20.	Scanning electron microscopy, energy dispersive spectrum X-ray analysis (EDS-SEM) of the spines of a cleavage stage sporangium, accelerating voltage of 15 keV	24
21.	The initial advancement of cleavage furrows (CF) during early cleavage	26
22.	The initial advancement of cleavage furrows (CF) during early cleavage	26

Page Page	ge
23. At mid-cleavage the cleavage furrows (CF) ramified throughout the sporangium, and isolated the spore protoplasts	7
24. The cleavage furrows (CF), isolating the spore protoplasts (SP), contain an electron translucent matrix and are lined with fusing electron opaque granules (arrow heads)	7
25. The cleavage furrows exhibit (1) the plasma membrane, (2) an electron translucent layer, (3) a layer of fusing electron opaque granules, (5) an electron transparent layer, and (6) an electron translucent granular matrix (layer (4) is defined latter)	7
26. Isolated spore protoplasts within a early postcleavage sporangium, separated by a matrix (M) of electron translucent material	9
27. Isolated spore protoplasts within a early postcleavage sporangium, separated by a matrix (M) of electron translucent material	9
28. Isolated spore protoplasts, note mitochondria (Mt), nuclei (N), and lipids (L)	0
29. (1) the spore protoplast plasma membrane,	0
30. (1) the spore protoplast plasma membrane,	0

igures Pa	age
31. The author's visualization of the ultrastructural transition from cleavage furrows isolating spore protoplasts (I), to post cleavage spores (II)	31
32. Postcleavage sporangium with mature spines and an furrow (arrows) at the base of the sporangium indicating the internal columella	34
33. The base of an unattached postcleavage sporangium, looking up through the sporangiophore (Sph)	34
34. The mid-postcleavage sporangium with dense spores (S), a thinning electron translucent matrix between the spores, and a widening electron transparent zone (ET)	35
35. The electron translucent matrix (M) closely oppressed to the fibrillar columellar wall, and the electron transparent zone (ET) surrounding the spores	35
36. Electron opaque granular bodies (Gb) which appear in the region just outside of the columella (Col)	35
37. A cross section of the very base of the sporangium, exhibiting the ultrastructural differences between the fibrillar columellar wall (CW) and the sporangial wall (SW)	35
38. Crossection of a late postcleavage sporangium showing the how the mature spores were displaced during specimen preparation	37
39. Higher magnification of Fig. 38 showing numerous vesicles (V) within the sporangium, arrow heads indicate vesicles fusing with the columellar plasma membrane	37
40. Mature spores within late postcleavage sporangia, and deliquescence of the sporangial wall	39

Figures Pa	ıge
41. Mature spores within late postcleavage sporangia, and deliquescence of the sporangial wall	39
42. Mature spores within late postcleavage sporangia, and deliquescence of the sporangial wall	19
43. The mature spore wall: (1) the spore plasma membrane, (2) a secondary spore wall layer, (3) two outer electron opaque wall layers, with a denser central interface layer (indicated by the arrows), (4) an electron translucent layer	39
44 Sporangial wall deliquescence and mature spore release 4	Ю
45 Sporangial wall deliquescence and mature spore release 4	ŀO
46. Mature sporangiospore release and sporangial wall collapse 4	12
47. Mature sporangiospore release and sporangial wall collapse 4	12
48. Complete sporangial degradation, and initiation of columellar collapse 4	13
49. Complete sporangial degradation, and initiation of columellar collapse 4	13
50. Microsporangia (bar = 10μ m)	14
51. A rare branching of a sporangiophore (bar = $10\mu m$)	14
52. <u>Zygorhynchus heterogamus</u> . An illustrative diagram of five proposed methods of spore wall formation 4	19

LIST OF ABBREVIATIONS

```
CF
     Cleavage Furrow
Col
          Columella
CV
     Cleavage Vesicle
DM
     Degenerate Mitochondria
ER
     Endoplasmic Reticulum
ET
     Electron Transparent
G
     Granule
Gb
     Granular Body
L
     Lipid
M
     Matrix
Mt
     Mitochondria
N
     Nucleus
R
     Remnants of secondary sporangial wall layer
S
          Spores
Sp
     Spines
SP
     Spore Protoplasts
Sph
          Sporangiophore
SW
     Sporangial Wall
V
          Vesicle
Va
     Vacuolar Granule
VR
     Vacuolate Region
```

Introduction

The culturing of members of the fungal order Mucorales on artificial media is one of the most common of all laboratory culturing practices; whether as the isolation of air-borne soil-inhabiting microorganisms, or as contaminants of other axenic cultures and even more commonly, as contaminants of baked goods, foods, and many other stored items. Amongst the Mucorales, as defined by Hesseltine and Ellis (1973) seven modes of reproduction have been defined. Of these six are defined as modes of anamorphic reproduction, consisting of (1) multispored sporangia, (2) few-spored sporangiola, (3) uni-spored sporangiola on vesicles, (4) few-spored merosporangia, (5) uni-spored merosporanigia, and (6) azygospores. The seventh mode is a teleomorphic reproduction via zygospores. these reproductive types, the first five provided a basis for Cole and Samson (1979) to taxonomically regroup such fungi into the Mucorales and Kickxellales. Further. Benjamin (1979) proposed a narrow arrangement of these fungi, distributing the taxa included in the Mucorales by Hesseltine and Ellis (1973) among the Mucorales, Kickxellales, Dimargaritales, and Zoopagales.

Consistently within such various taxonomic arrangements the Mucorales has retained those fungi producing multispored sporangia. Of this group producing multispored sporangia, the ultrastructural development of the sporangia and sporangiospores of only two fungal species have been previously described. In 1966, later expanded in 1968, Bracker described sporangiosporogenesis in Gilbertella persicaria (Eddy) Hesseltine, and, in 1981, Hammill described sporangiosporogenesis in Mucor mucedo L.: Fr.. Based on his work with G. persicaria, Bracker established the currently accepted model of development in multispored sporangia (Fig. 1).

Hammill (1981) modified Bracker's model and summarized the developmental sequence of events of sporangiosporogenesis combined into one diagram (Fig. 1), and divided these events into three major stages: A (precleavage), B (cleavage), and C (postcleavage). These three major stages were then further subdivided into early, mid-, and late cleavage events. These stages were ultrastructurally detailed in G. persicaria by Bracker (1966, 1968) as follows.

Figure 1. Diagram (reprinted from Hammill, 1981) summarizing the process of sporangiospore formation in G. persicaria. Only the cleavage apparatus and walls are indicated. Spatial distribution of developmental stages is convenience in illustration only, and does not represent spatial progression within a single sporangium. STAGE A: PRECLEAVAGE. Early precleavage (I-II), mid-precleavage (III), late precleavage (IV). STAGE B: CLEAVAGE. Early cleavage (V), mid-cleavage (VI), late cleavage (VII). STAGE C: POSTCLEAVAGE. Early postcleavage (VIII), midpostcleavage (IX), late postcleavage or spore maturity (X). The discontinuity in the sporangial wall near X represents rupturing of the sporangium as it splits into two halves at maturity.

The Brackerian Model

The precleavage sporangia (Fig. 1, A I-IV) contained a cytoplasm matrix very similar to that of the vegetative hyphae (nuclei, endoplasmic reticulum (ER), mitochondria, lipid bodies, vacuoles, microbodies). Although no mitotic nuclei were observed within the sporangial apparatus, numerous nuclei were observed interconnected by ER. Two types of early precleavage sporangia were observed, one with few cytoplasmic vesicles and one with many small vesicles, the latter was believed to be a later stage (Fig. 1, A I & II). The vesicles, $0.1-0.2\mu m$ in diameter, were found mainly near the top periphery of the sporangium and were generally closely associated with ER. Bracker stated that these vesicles arose from cisternal rings (fungal structures proposed to be similar in function to the goldi apparatus).

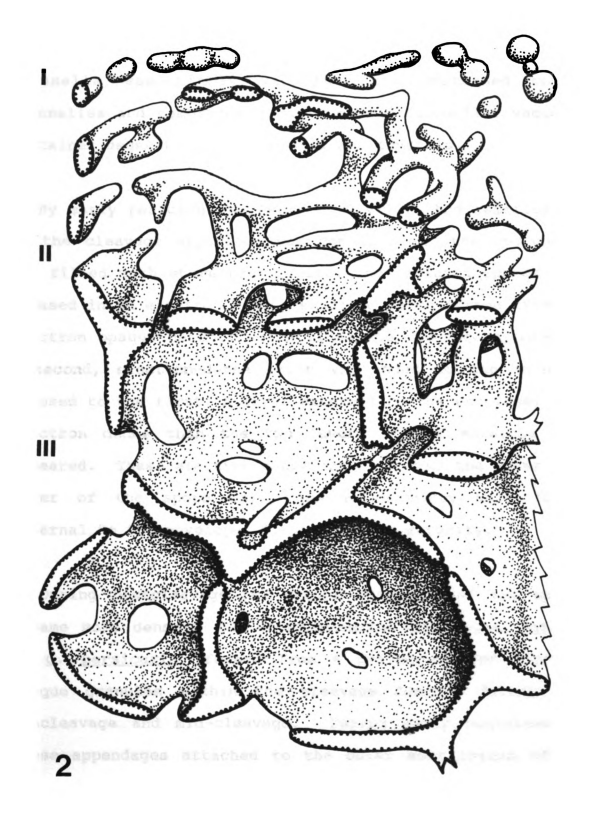
By mid-precleavage (Fig. 1, A III), the small vesicles fused to form larger vesicles which were surrounded by a cage of ER. These larger vesicles contained small electron opaque granules, 8-20nm, around their inner surface, 8nm from the vesicular plasma membrane. These granules were used as markers identifying cleavage vesicles and cleavage furrows. Rarely were the granules seen scattered throughout the cleavage vesicles. By late precleavage (Fig. 1, A IV)

these cleavage vesicles were found throughout the entire sporangium.

At early cleavage (Fig. 1, B V), these cleavage vesicles fused to form cleavage furrows. At this time numerous cisternae were observed which contained poorly developed granules. Elongation and branching of the cleavage furrows marked the transition from early cleavage to mid-cleavage within the sporangium (Fig. 1, B V & VI). Initial extension of the cleavage furrows occurred through the fusion of cleavage vesicles. Although within individual sporangia several stages of the fusion of vesicles could be observed, Bracker stated that cleavage occurred more-or-less simultaneously throughout the sporangium. By late cleavage (Fig. 1, B VII), the cleavage furrows ramified throughout the sporangium, isolating units of the sporangial matrix, forming a unified, three dimensional cleavage apparatus (Fig. 2). Advancement of the cleavage furrows, after the initial stages, was believed to have occurred through extension rather than by the addition of new vesicular material. During late cleavage the individual granules of the cleavage furrows begin to fuse together forming an electron opaque network lining the cleavage furrows, 8nm from the membrane.

During cleavage, the columellar region (Fig. 1, B VI

Figure 2. Cutaway three-dimensional interpretive drawing (reprinted from Bracker, 1968) showing the author's concept of the cleavage apparatus during early cleavage (I), mid-cleavage (II), and late cleavage (III).



VII, COL) was delimited from the rest of the sporangium by a dome of vesicles which aligned near the base of the sporangium and fused in a process morphologically identical to that which delimited the spores. The interior of the columella was highly vacuolate and contained common organelles and membranes. The numerous columellar vacuoles contained degenerate mitochondria and crystals.

By early postcleavage (Fig. 1, C VIII), the ramification of the cleavage apparatus was complete and the sporangium was filled with spore protoplasts. The isolated spores were encased in an electron opaque envelope which formed from the electron opaque network which lined the cleavage apparatus. A second, electron-dense layer was added to the envelope apposed to the first. A layer external to the envelope, less electron dense than the two layers of the envelope also appeared. These electron dense layers formed the outer most layer of the spore wall, and a secondary wall formed internal to the envelope, $0.4\mu m$ thick at maturity.

During postcleavage the ground cytoplasm of the spores became more dense. The sporangiospore appendages, typical of <u>G. persicaria</u>, formed from a coalescence of electron opaque granules within the cleavage furrows during late precleavage and mid-cleavage. During early postcleavage, these appendages attached to the outer most layers of the

spore wall. Spore release occurred through the rupture of the sporangial wall.

Hammill (1981) found that sporangiosporogensis in Mucor mucedo occurred very similarly to that described by Bracker (1966, 1968) for Gilbertella persicaria as summarized above, with the following exceptions. Bracker found that the cisternal rings decreased in number in G. persicaria during mid-cleavage, in M. mucedo they were found in all stages, and functioned in the addition of new material to the advancing cleavage apparatus and may have been involved in spore wall synthesis. Hammill (1981) observed no electron opaque granules in the cleavage vesicles or cleavage furrows of M. mucedo. Hammill, however, did observe an amorphous electron dense material within the matrix of the cleavage vesicles and cleavage furrows. He proposed that this material coalesced to form an electron opaque surrounding the spore protoplasts, in late cleavage and early postcleavage, resulting in an electron opaque outer layer of the mature spore walls. Unlike Bracker's observation of an absence of mitotic nuclei within the developing sporangia of G. persicaria, Hammill frequently observed mitotic nuclei during sporangial initiation of M. Hammill also observed numerous autophagic vacuoles mucedo. within columellae of M. mucedo and believed them to be similar to the vacuoles found in the columellae of \underline{G} .

persicaria by Bracker.

For this study, Zygorhynchus heterogamus Vuillemin, was selected for several reasons. The ultrastructural development of sporangiosporogenesis of a third representative genus of the Mucorales provides a better foundation for an overall understanding of multispored sporoangiosporogenesis within the Mucorales. Zygorhynchus heterogamus is the type species of the genus, and was viewed as the representative species of homothallic zygospore formation in the Zygomycetes. The description of the ultrastructural development of sporangiosporogenesis provides a basis for the description of the ultrastructural development of the complete life-cycle of such representative of homothallic zygospore reproduction. Additionally Z. heterogamus readily forms multispored sporangia in culture, and is easy to maintain in culture.

Materials and Methods

Cultures

A culture of Zygorhynchus heterogamus Vuillemin, was obtained from E. S. Beneke and A. L. Rogers (Department of Botany and Plant Pathology, Michigan State University), and keyed out to verify species identification (Hanlin, 1973, Hesseltine, et. al., 1959, Domsch, et. al., 1980). Subcultures were grown and maintained on a 2% V-8 juice agar consisting of 177 ml V-8 juice (Campbell Soup Company, Camden, N.J.), 2 gm calcium carbonate, 20 gm Bacto-Agar (Difco Laboratories, Detroit, Mi.), and 800 ml deionized water. Cultures were incubated at 22-24 °C, with a photoperiod of 12 hr light/ 12 hr dark in a Precision Scientific (model 805) incubator. Cultures were grown for 3-6 days and prepared for observation at all stages of sporangial development.

Scanning Electron Microscopy

Specimens for scanning electron microscopy (SEM) were grown as above and fixed and dehydrated as follows: blocks of agar, 5mm x 5mm, were cut, using a razor blade, from areas of growing colonies containing the desired stages of

sporangial development. These specimen blocks were then quickly immersed for 20-30 min at 22°C, in glutaraldehyde, and 1.0% paraformaldehyde in an aqueous solution buffered by 0.05 M sodium cacodylate at pH 7.2, and osmotically balanced by 1% sucrose, with 5 drops Tween 20 / 1.5ml, as a wetting agent. Primary fixation was followed by a 2-3hr rinse with several complete changes of the same balanced buffer. Secondary fixation was carried out using 1.0% osmium tetroxide in the same balanced buffer for 4-5hr at room temperature, followed by a rinse for 1hr in several changes of distilled water. Specimens were dehydrated using a graded ethyl alcohol series of 25% (30min), 50% (30min), 75% (30min), 85% (30min), 95% (1hr), 100% (1hr), 100% (1hr), followed by critical point drying using liquid carbon dioxide as the transition fluid in a Balzers Union FL-9496 critical point drying unit.

Dried and fixed specimens were mounted on aluminum stubs, using adhesive tabs, (M.E. Taylor Engineering Inc., Brookeville, Md.) grounded with silver paint (Ladd, co.) and coated with approximately 25nm of gold using an Emscope SC 500 sputter coater. Specimens were observed using a JEOL 35 CF scanning electron microscope, with an accelerating voltage of 10 keV. Micrographs were obtained using Polaroid 665 positive/negative film, processed according to manufacturer's procedures.

Transmission Electron Microscopy

Specimens for transmission electron microscopy (TEM) were grown as above, fixed and dehydrated as follows: blocks of agar, 2.5mm x 2.5mm x 2.5mm, were cut, using a razor blade, from areas of growing colonies containing the desired stages of sporangiospore development. specimen blocks were quickly immersed in a primary fixation solution of 2.5% glutaraldehyde, and 1.0% paraformaldehyde in an aqueous solution buffered by 0.05M sodium cacodylate at pH 7.2, and osmotically balanced by 1% sucrose, with 5 drops Tween 20 / 1.5ml, as a wetting agent for 20-30min at 22°C. Primary fixation was followed by a 2-3hr rinse with several complete changes of the same balanced buffer. Secondary fixation was carried out using 1.0% osmium tetroxide in the same balanced buffer for 4-5hr at room temperature, followed by a second rinse for 1hr in several changes of distilled water. Specimens were then en bloc stained overnight (12-16hr) using 0.5% aqueous uranyl acetate followed by a rinse for 1hr in several changes of distilled water.

Specimens were dehydrated using a graded ethyl alcohol series of 25% (30min), 50% (30min), 75% (30min), 85% (30min), 95% (1hr), 100% (1hr), 100% (1hr), followed by

graded infiltration and embedment into Spurr's (1967) ERL epoxy resin. The Spurr's resin was prepared with 10.0gm ERL-4206 (vinyl cyclohexene dioxide), 4.0gm DER 736 (diglycidyl ether of propylene glycol), 26.0gm NSA (nonenyl succinic anhydride), and 0.4gm DMAE (dimethylamino-ethanol). Infiltration with Spurr's resin was carried out in three steps: 3:1 ethyl alcohol to Spurr's resin (3hr with one change), 1:1 ethyl alcohol to Spurr's resin (3hr with one change), followed by three (3hr each) changes of 100% Spurr's. Specimens were polymerized in flat embedding molds at 65°C for 60-65hr.

Polymerized blocks were first examined using a Wild light microscope in order to identify suitable sporangial specimens, and the surface of the blocks were inscribed with a dissecting needle to mark specimen location. Ultrathin sections (50-80nm thick) of these appropriate specimens were prepared using a Sorval MT-2 ultramicrotome and a diamond knife (Delaware Diamond knives). Sections were picked up on collodion-coated, 100 mesh, copper grids. Sectioned specimens were post-stained using 0.5% uranyl acetate (25 min), rinsed with distilled water, followed by Reynold's lead citrate (1963) (10 min), rinsed with 0.02 N sodium hydroxide, and a final distilled water rinse. Specimens were observed and photographed using a JEOL 100CX II TEM at an accelerating voltage of 80 keV.

X-ray Analysis

specimens for both SEM and TEM were analyzed using energy dispersive spectroscopy (EDS) in order to determine major elemental deposits, in particular the conspicuous sporangial spines found on maturing sporangia. The SEM-EDS specimens were prepared as stated previously for SEM, except that they were coated with approximately 30 nm of carbon, instead of gold. The SEM-EDS was carried out using a JEOL 35c SEM with a Tracor Northern TN2000 X-ray analyzer. The TEM-EDS specimens were prepared as previous for TEM, except that secondary fixation with osmium tetroxide, en bloc staining with uranyl acetate and all post-section staining were not performed, and thin (150-180nm) sections on grids were coated with approximately 30 nm of carbon. The TEM-EDS was carried out using a JEOL 100CX II TEM with a LINK Systems AN10000 X-ray analyzer.

Light Microscopy

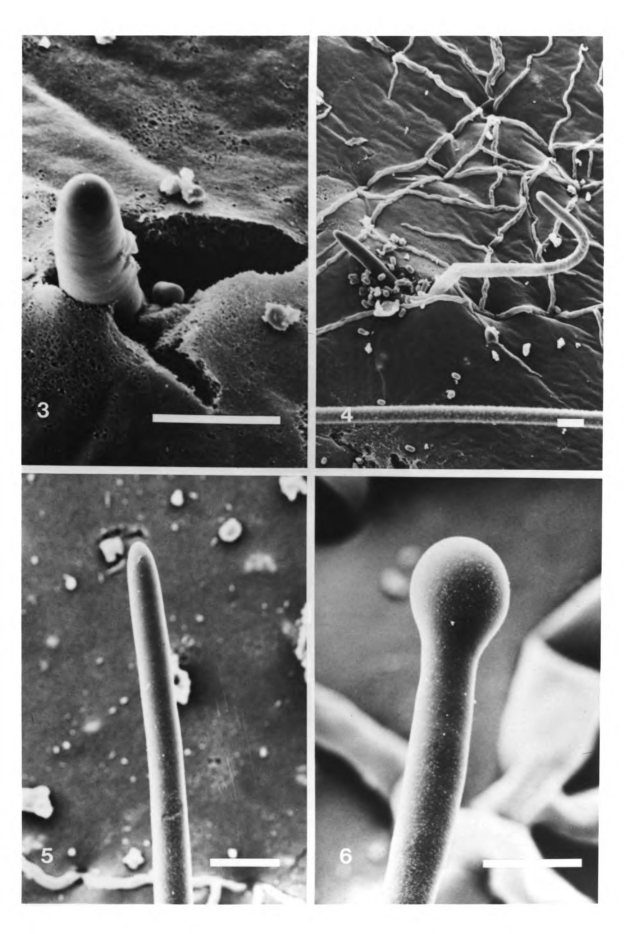
Mature spores were harvested, cleared and stained, using a modified technique of Hammill and Secor (1983) in order to determine the number of nuclei. Ten day old cultures were flooded with a modified Helly's fixative, containing freshly prepared 5% HgCl₂, 3% K₂Cr₂O₇, and 0.2% paraformaldehyde in

water, and were subsequently washed into test tubes which were incubated at 43°C for 40min. The spores were centrifuged, resuspended in 70% ethanol, and followed with three repeated centrifugations and resuspensions deionized water. Concentrated spore suspensions were airdried and heat-fixed onto glass microscope slides for 2hr using a 50°C slide warming tray. Prepared slides were hydrolyzed for 20min in 1N HCl at 60°C. Slides were stained for 10min in hematoxylin, rinsed 1-2min in deionized water, dipped twice into an aqueous 2% ammonium hydroxide solution, rinsed 1-2min in deionized water, decolorized in acid alcohol (70% ethanol and 1% HCl), and rinsed 1-2min in deionized water. Cover slips were mounted with water, ringed with clear nail polish to retard drying, and observed using a Zeiss light microscope under oil at 1000x.

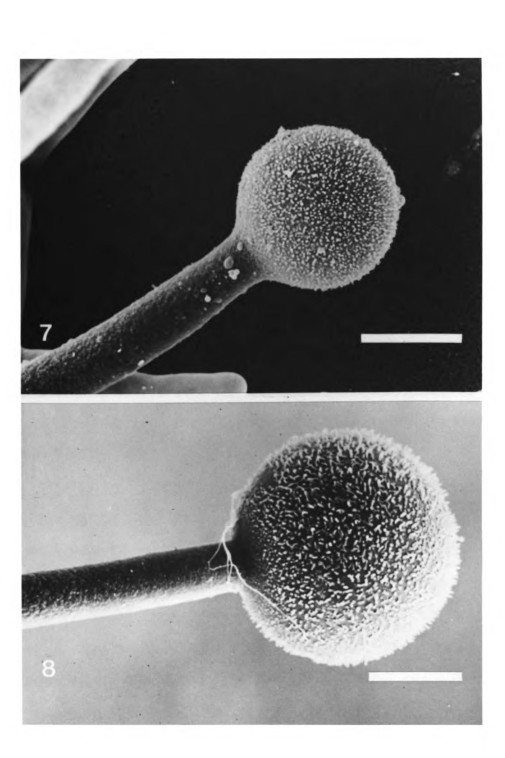
Results

Precleavage

Identifiable sporangial apparatus initiation occurred when the sporangiophore rapidly ruptured through the substrate surface (Fig. 3). The sporangiophore was continually supplied by a network of substratum vegetative mycelia. Sporangiophore initials were identified as developing sporangiophores by their vertical aerial development, and uniform, large, 7-10 μ m, diameter. vegetative hyphae and developing zygophores were narrower, 1-6 μ m and 5-8 μ m respectively, rapidly twisted, branched, and maintained a more inclined angle of growth. The sporangiophore rapidly extended uniformly, very rarely branching, for 0.5-1.4mm, maintaining a blunted growing apex (Figs. 4 & 5). The apex ballooned outward (Fig. 6) becoming filled with a highly vacuolate cytoplasm containing numerous nuclei interconnected with a vigorously expanding network of endoplasmic reticulum (Figs 7-13). The force of this influx was observed as an elongation of the various organelles inside the sporangiophore and just inside the neck of the developing sporangium (Fig. 9). Such an elongation of organelles was not observed at the periphery of sporangia at Figures 3-6. Early precleavage. 3. Rupture of the sporangiophore through the agar substrate (bar = 10μ m). 4. Aerial sporangiophore elongation (bar = 10μ m). 5. Straight, unbranched sporangiophore elongation prior to sporangial swelling (bar = 10μ m). 6. Initiation of sporangial swelling (bar = 10μ m).



Figures 7 & 8. Mid- and late precleavage. 7. Sporangial swelling and initiation of spine formation during mid-precleavage (bar = 10μ m). 8. Late precleavage sporangial swelling and spine elongation with and absence of spines near the sporangial base (bar = 10μ m).

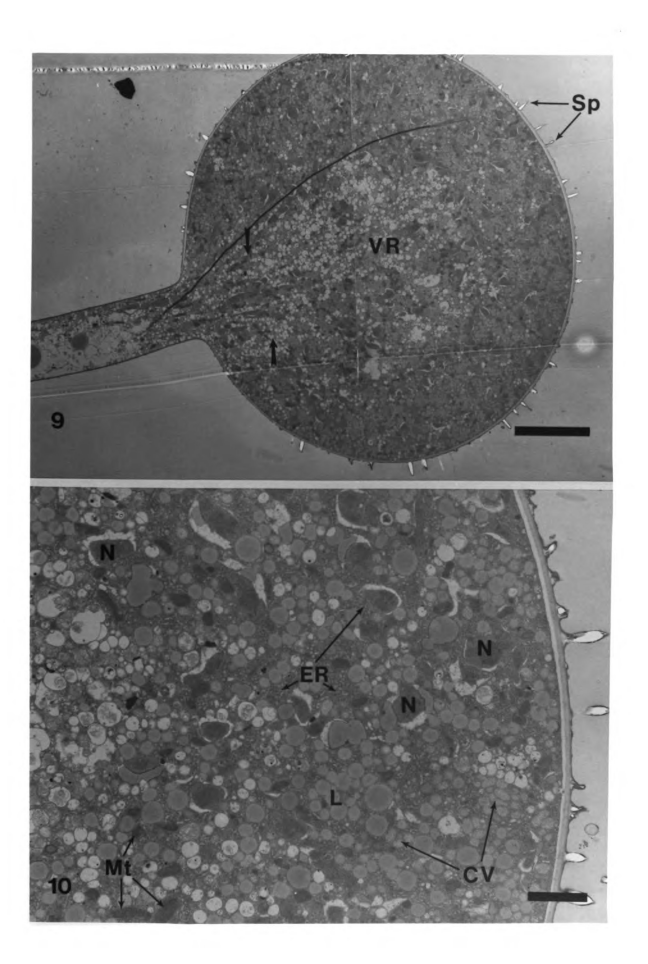


this stage (Fig. 10 & 11), anywhere within later sporangia (Figs. 14-42), nor within vegetative hyphae. At this early precleavage stage, no nuclear division was observable and it is believed that mitotic nuclear division occurred prior to sporangium formation and/or lower in the sporangiophore. Even at this very early precleavage stage, in the periphery of the sporangium numerous cleavage vesicles were recognized by the electron opaque granules within them (Figs. 11-13).

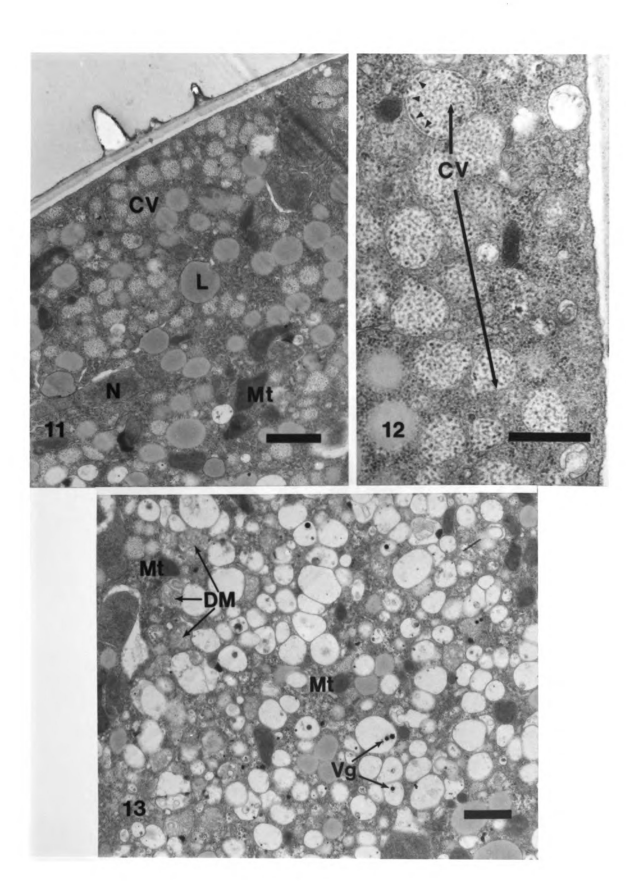
From early precleavage through to late precleavage a definite decrease in the number of mitochondria within the developing sporangium was observed. Early precleavage sporangia, (Figs. 9-13), showed numerous densely staining mitochondria which were easily recognizable by their typical internal lamellae (Figs. 10-12). Commonly present in central regions of the same sporangial sections were numerous double membrane-bound, membrane-filled structures which appeared to be degenerate mitochondria (Figs. 13 & 15). Such degenerate mitochondria could readily be found in all states of degeneration, from easily recognizable, though non-densely staining, to membrane-bound structures containing disorganized layers of membranes (Fig. 15). Late precleavage sporangia were found to contain few, if any, densely-staining mitochondria (Figs. 14 & 15).

Shortly after the induction of sporangium expansion,

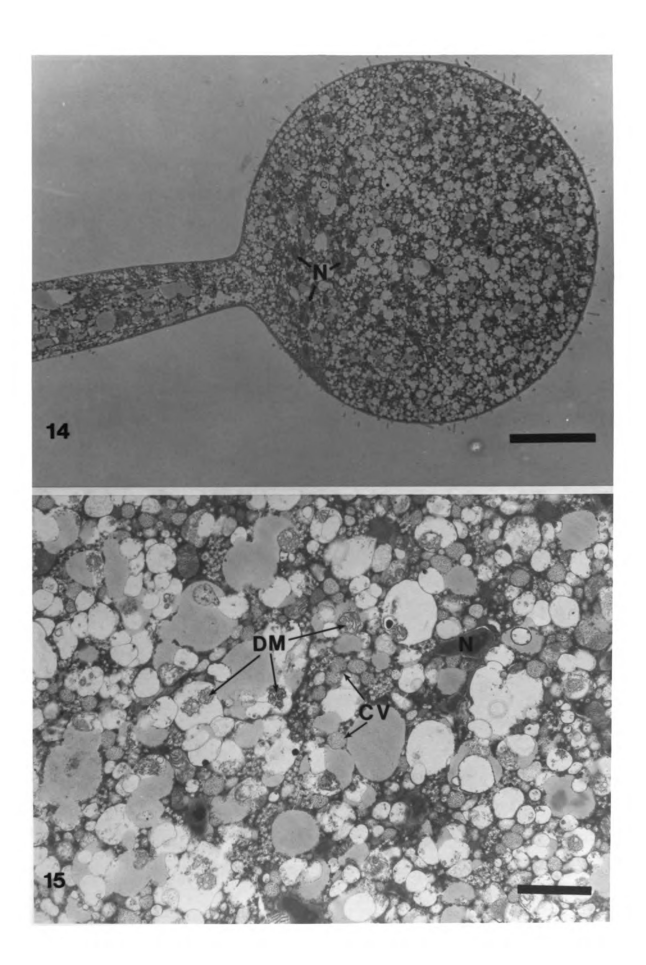
Figures 9 & 10. Mid-precleavage. 9. Sporangium with a central vacuolate region (VR), and a denser periphery. Arrows indicate a zone of elongated organelles between the sporangiophore and sporangium suggesting an indication of a rapid transport of material into the sporangium. Spines (Sp) are attached to the outer sporangial wall layer (bar = $10\mu\text{m}$). 10. The sporangial cytoplasm shows nuclei (N) closely associated with an interconnecting network of endoplasmic reticula (ER), mitochondria (Mt), and lipids (L). Numerous cleavage vesicles (CV) are shown within the sporangial periphery (bar = $2\mu\text{m}$).



Figures 11-13. Mid-precleavage. 11. The denser sporangial peripheral cytoplasm contains numerous cleavage vesicles (CV) containing electron opaque granules, along with nuclei (N) closely associated with ER, mitochondria (Mt), and lipids (L) (bar = 1μ m). 12. Mid-precleavage cleavage vesicles (CV), which contained an electron opaque granular matrix, exhibited the characteristic alignment of electron opaque granules along their periphery (indicated by the arrow heads) just inside the cleavage vesicle plasma membrane. At this stage the initiation of the fusion of the these granules began (bar = 0.5μ m). 13. The central vacuolate region exhibits typical mitochondria (Mt) as well as degenerate mitochondria (DM), and vacuoles containing crystalline granules (Vg) (bar = 1μ m).



Figures 14 & 15. Late precleavage. 14. At this stage the sporangial matrix appears uniformly vacuolate, note nuclei (N) (bar = 10μ m). 15. The sporangial matrix shows a general distribution of cleavage vesicles (CV). Numerous degenerate mitochondria are seen in all stages of degeneration, with an absence of "typical" mitochondria (bar = 1μ m).



exterior surface of the sporangium (Figs. 7, 8 & 16). These spines persisted in their attachment to the outer layers of the sporangial wall (Figs. 10), and were maintained to the point of sporangial wall dissolution.

Only three, subtle external features were noted which distinguished precleavage and cleavage sporangia; (1) the base of the cleavage sporangium was encircled by a shallow depression, indicating the presence of the columella which formed during cleavage (Fig. 19), (2) the spines were found to spread down to the very base of the external wall of the sporangium by mid to late cleavage (Figs. 16-19), (3) and a change in the area between the sporangiophore and the sporangium from a gradual curve to a sharp angle at the very base of the sporangium. This area was associated with a fine ring (Figs. 16-19). Using the SEM and X-ray microanalysis, the spectra of the spines showed a predominance of calcium (Fig. 20), most likely calcium oxalate.

Cleavage

Formation of the sporangiospores from the general sporangial cytoplasm occurred through the three-dimensional ramification of a network of cleavage furrows which isolated discrete units of cytoplasm. The interior of the individual

Figures 16-19. Late precleavage through late cleavage. 16. Early cleavage sporangium with elongated spines (bar = $10\mu m$). 17. Late precleavage sporangium with shorter spines, spineless sporangial base (double ended arrow), and smooth transition (arrows) from sporangiophore to sporangium (bar = $1 \mu m$). 18. Early cleavage sporangium with a right angle transition from sporangiophore and sporangium (arrow) (bar = $10\mu m$). 19. Late cleavage sporangium with grooved ring (arrows) indicating the presence of an internal columella. Characteristic ring marking transition from sporangiophore to sporangium, elongated spines with narrow spineless area at the sporangium base (bar = $10\mu m$).

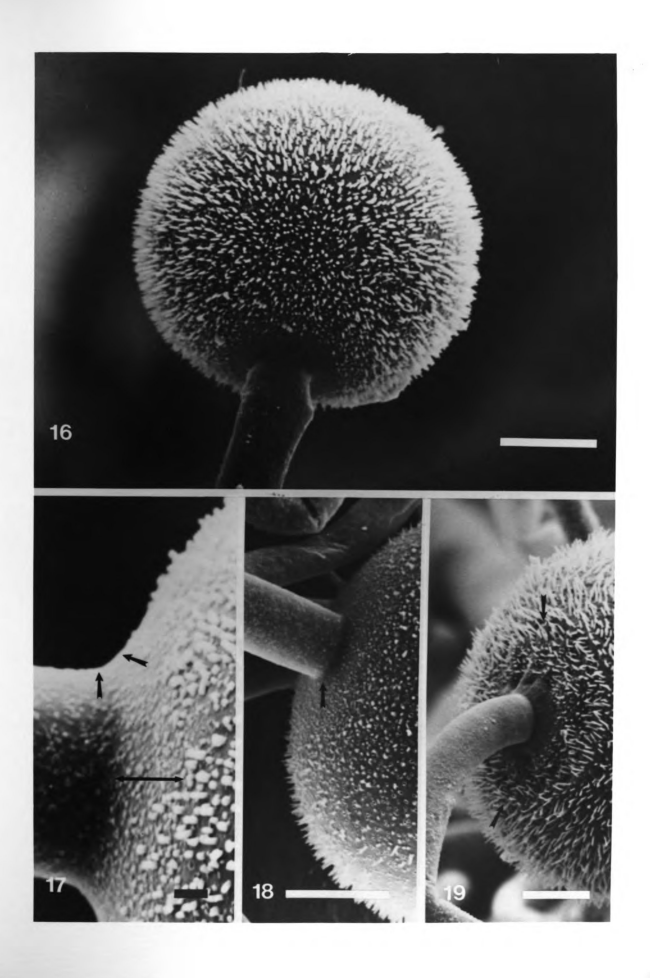
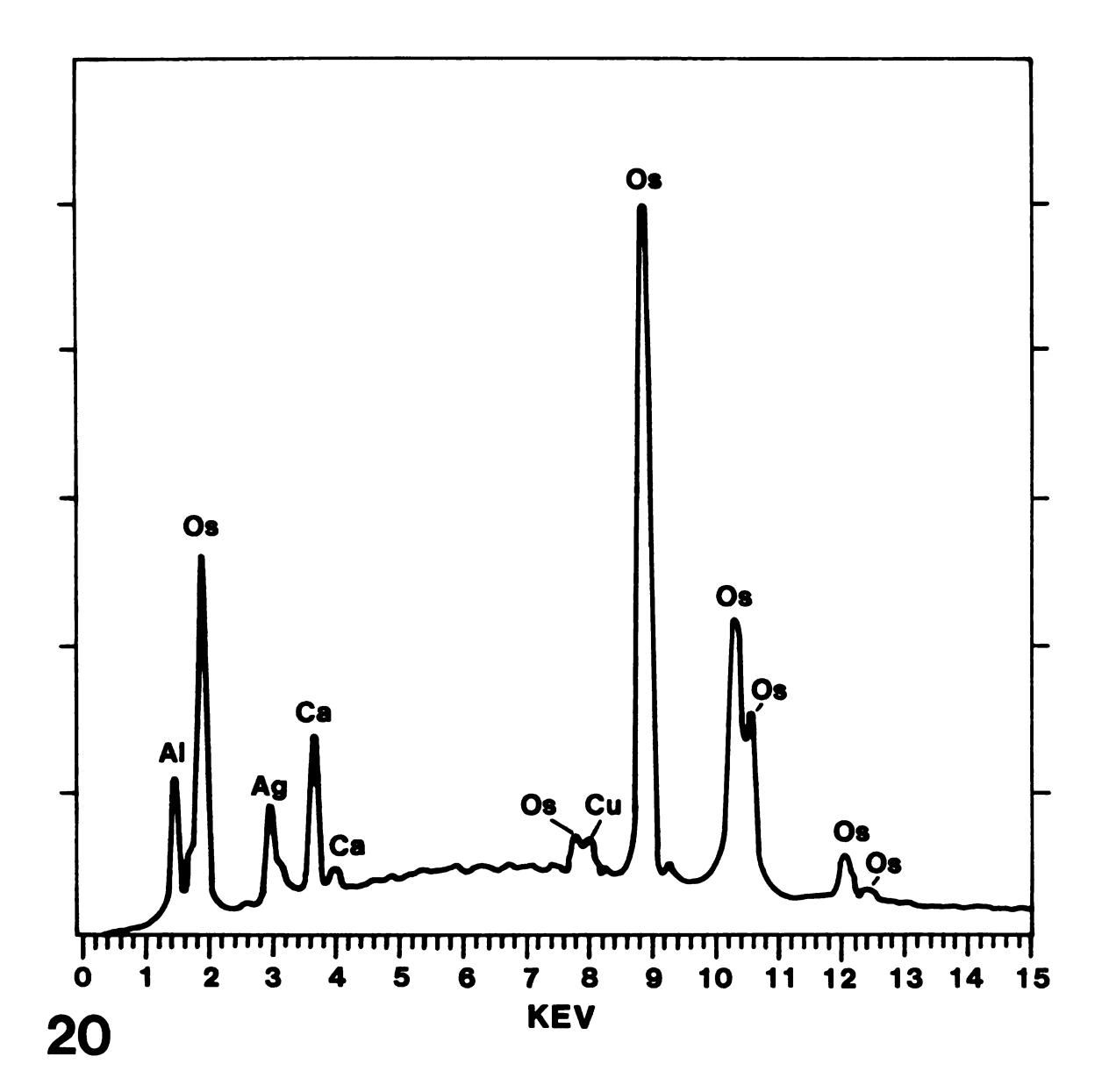
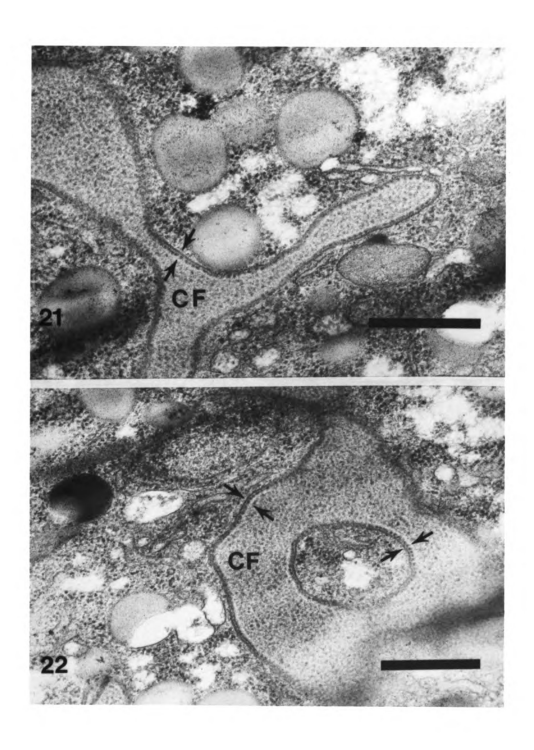


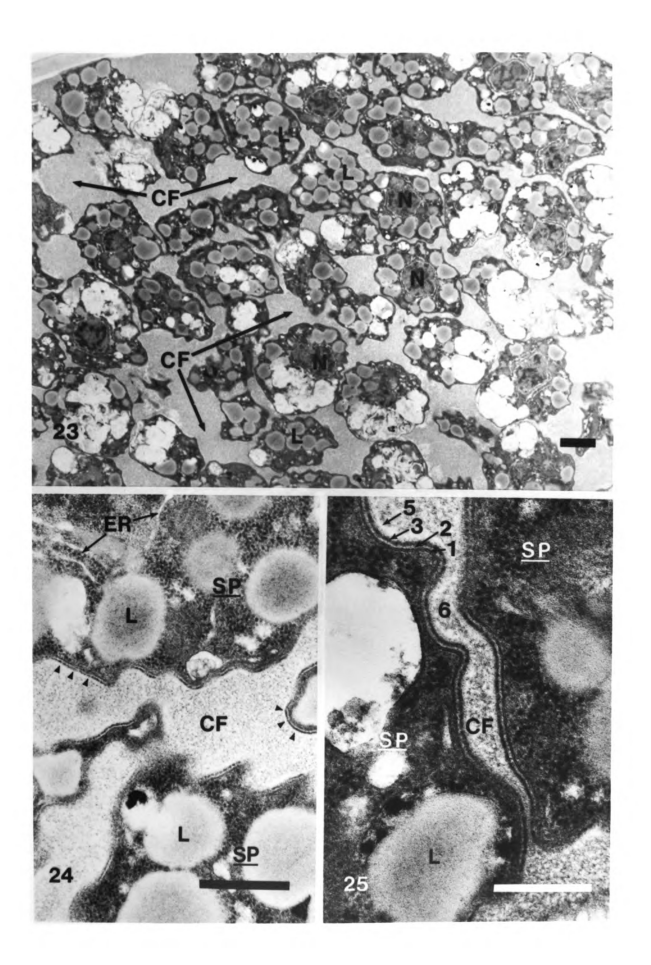
Figure 20. Scanning electron microscopy, energy dispersive spectrum X-ray analysis (EDS-SEM) of the spines of a cleavage stage sporangium, accelerating voltage of 15 keV. The major component of the spines was calcium (Ca). Aluminum (Al) was from the specimen mounting stub, osmium (Os) was due to specimen fixation, copper (Cu) is a system artifact of the detector, and silver (Ag) was used as a conductive ground between the specimen and the aluminum stub.



cleavage furrows were lined with electron opaque granules which fused to form a boundary layer completely surrounding the isolated regions of cytoplasm (Figs. 21-30). The coalescence of the electron opaque granules began in the first identifiable cleavage vesicles, for it was by the observation of electron opaque granules that cleavage vesicles were defined. Even at such early precleavage stages, a close association, if not fusion itself, between electron opaque granules was repeatably observed (Fig. 12). This fusion of electron opaque granules became more notable during mid-cleavage (Figs 21 & 22), and was a primary characteristic of late cleavage (Figs. 23-25). possible to identify five distinct regions of the cleavage furrows, the cleavage furrow plasma membrane (Fig. 25, 1); an electron translucent layer (Fig. 25, 2); a layer of fusing electron opaque granules (Fig 25, 3); a zone of electron transparency (Fig. 25, 5); and the fine electron translucent matrix of the cleavage furrow (Fig. 25, 6). The formation of a contiguous electron opaque layer, external to the newly formed spore protoplasts, via this fusion of separate electron opaque granules within the advancing cleavage furrows, was essentially simultaneous with the culmination of the process of spore excision. In general two nuclei (determined through light microscopy) closely associated with endoplasmic reticula and several large lipid globules, along with several vacuoles containing osmiophilic Figures 21 & 22. The initial advancement of cleavage furrows (CF) during early cleavage. The cleavage furrows exhibit a granular matrix, and a peripheral zone composed of the cleavage furrow plasma membrane, a layer of electron opaque granules, and an electron translucent layer (arrows) (bars = $0.5\mu m$).



Figures 23-25. Mid-cleavage. 23. At mid-cleavage the cleavage furrows (CF) ramified throughout the sporangium, and isolated the spore protoplasts (bar = 1μ m). 24. The cleavage furrows (CF), isolating the spore protoplasts (SP), contain an electron translucent matrix and are lined with fusing electron opaque granules (arrow heads) (bar = 0.5μ m). 25. The cleavage furrows exhibit (1) the plasma membrane, (2) an electron translucent layer, (3) a layer of fusing electron opaque granules, (5) an electron transparent layer, and (6) an electron translucent granular matrix (layer (4) is defined latter, bar = 0.5μ m).



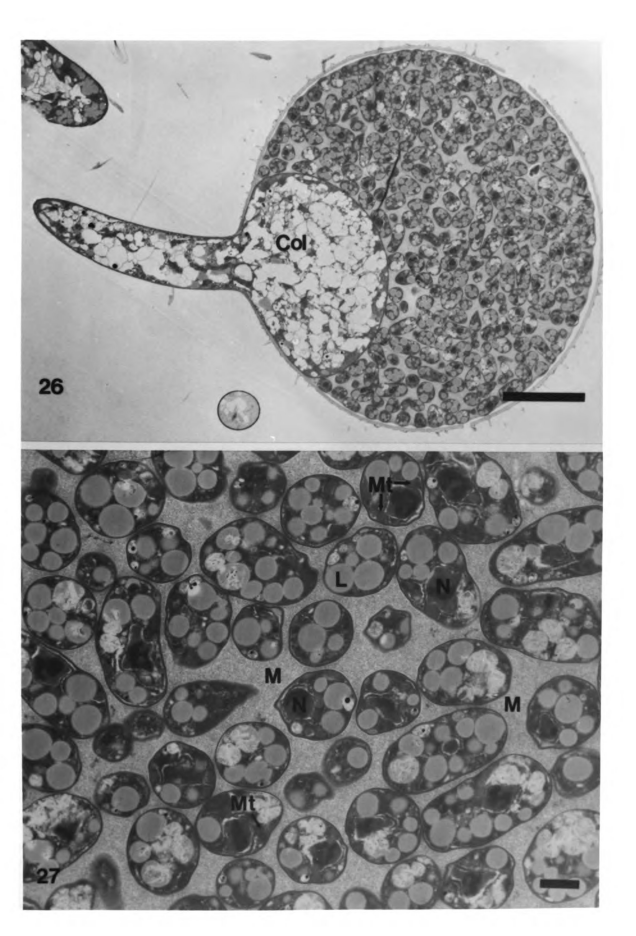
crystalline material, and glycogen-containing vesicles were isolated by the advancing cleavage furrows (Figs. 21-30), and became the major constituents of the newly formed spore protoplasts. At the latest stages of cleavage, and early stages of postcleavage, mitochondria were also able to be identified once again within the spore protoplast cytoplasm (Figs. 27 & 28).

Throughout mid-cleavage and late-cleavage, concurrent with the development of the cleavage furrows, there was a condensation of the cytoplasm isolated by the cleavage furrows (Figs. 21-30 & 34-36). Correspondingly, there was also an enlargement of the space between the future spores as defined by the cleavage furrows (Figs 21-30 & 34-36). Within these spaces a finely granular electron translucent matrix of material was found (Fig. 25, 6). It was this material which coalesced onto the exterior of the spore protoplasts forming the electron opaque outer layer of the spore wall.

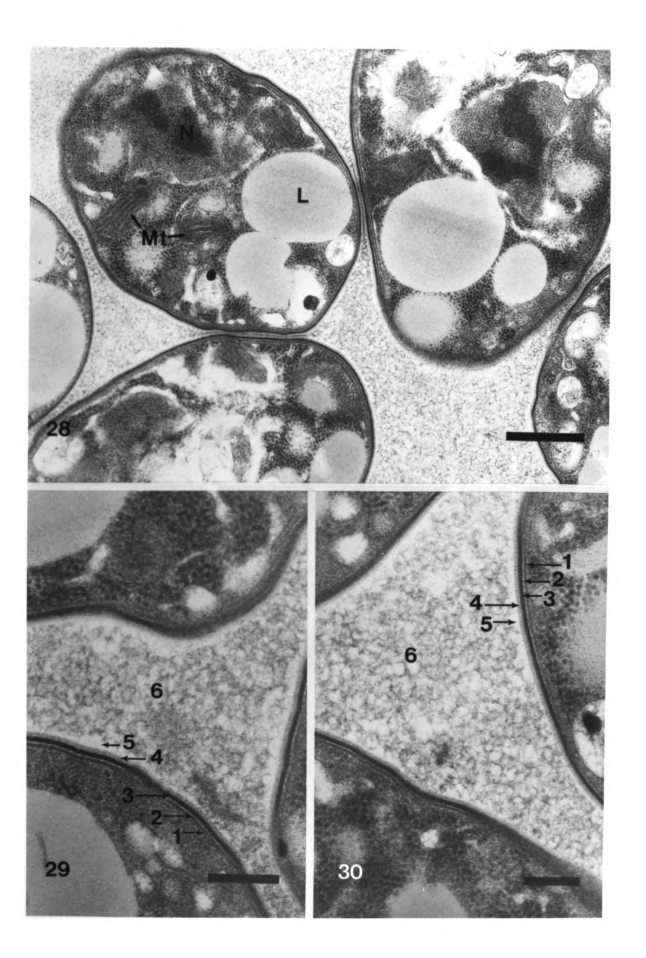
Postcleavage

At the initiation of postcleavage (Figs 29-33) six distinct regions could be defined for the area which would become the spore wall (Figs. 29 & 30). Proceeding from the

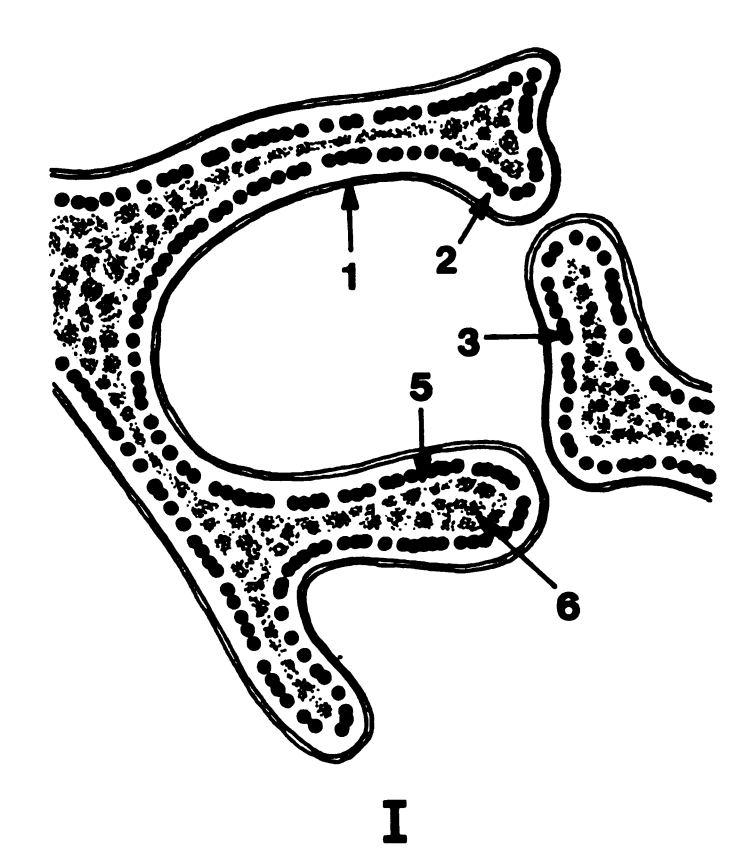
Figures 26 & 27. Isolated spore protoplasts within a early postcleavage sporangium, separated by a matrix (M) of electron translucent material. Note the columella (Col) at the sporangium base, and the reappearance of mitochondria within the cytoplasm of the isolated spore protoplasts. (26. bar = 10μ m, 27. bar = 1μ m).

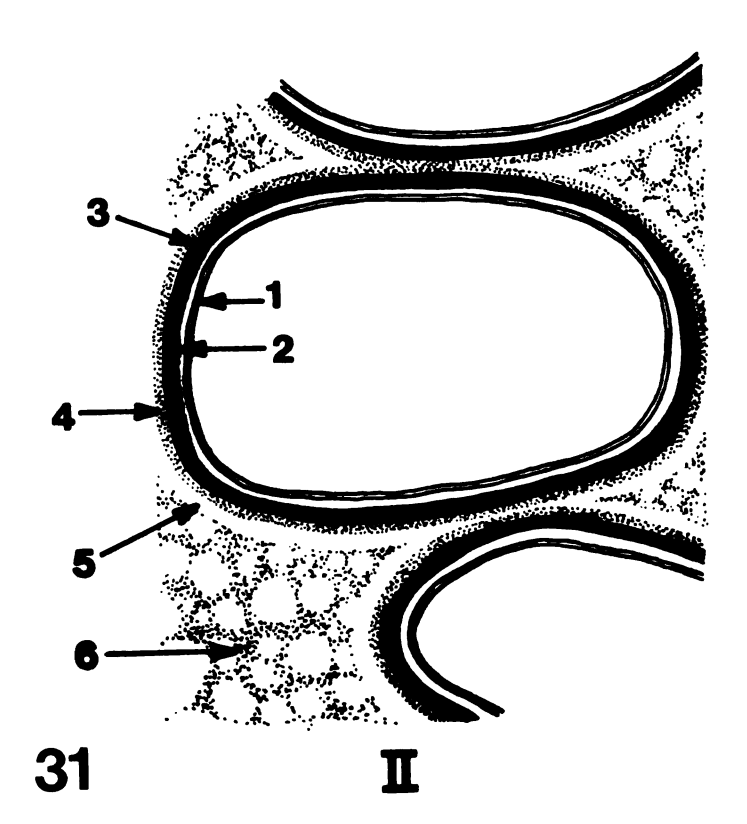


Figures 28-30. Early postcleavage. 28. Isolated spore protoplasts, note mitochondria (Mt), nuclei (N), and lipids (L) (bar = $0.5\mu m$). 29 & 30. (1) the spore protoplast plasma membrane, (2) an electron translucent layer, (3) the electron opaque layer, forming the outer spore wall layer, (4) an electron translucent transition layer, (5) an electron transparent layer, and (6) the electron translucent matrix between the spore protoplasts (29. bar = $0.1\mu m$, 30. bar = $0.2\mu m$).



The author's visualization of Figure 31. ultrastructural transition from cleavage furrows isolating spore protoplasts (I), to post cleavage spores (II). Only cleavage and wall forming structures are shown for STAGE I contains: (1) the cleavage furrow simplicity. plasma membrane, (2) an electron translucent layer, (3) a layer of fusing electron opaque granules, (5) a zone of electron transparency, and (6) the electron translucent matrix of the cleavage furrow. STAGE II contains: (1) the spore plasma membrane which was the cleavage furrow plasma membrane, (2) an electron translucent layer, (3) the electron opaque layer of the spore, which were the fusing granules of the cleavage furrows, (4) an additional electron translucent layer, which had no corresponding layer within the cleavage furrows, (5) a uniform zone of electron transparency, similarly placed in the cleavage furrows, and (6) a non-uniform granular matrix separating the spores.

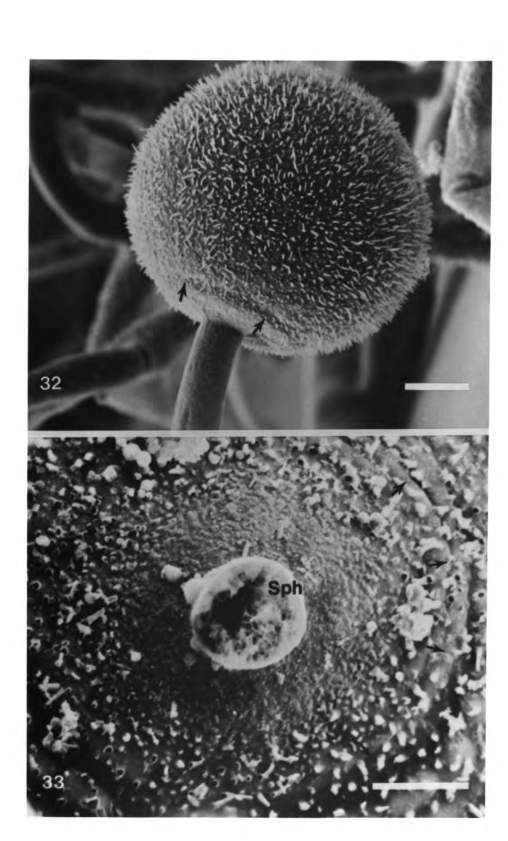




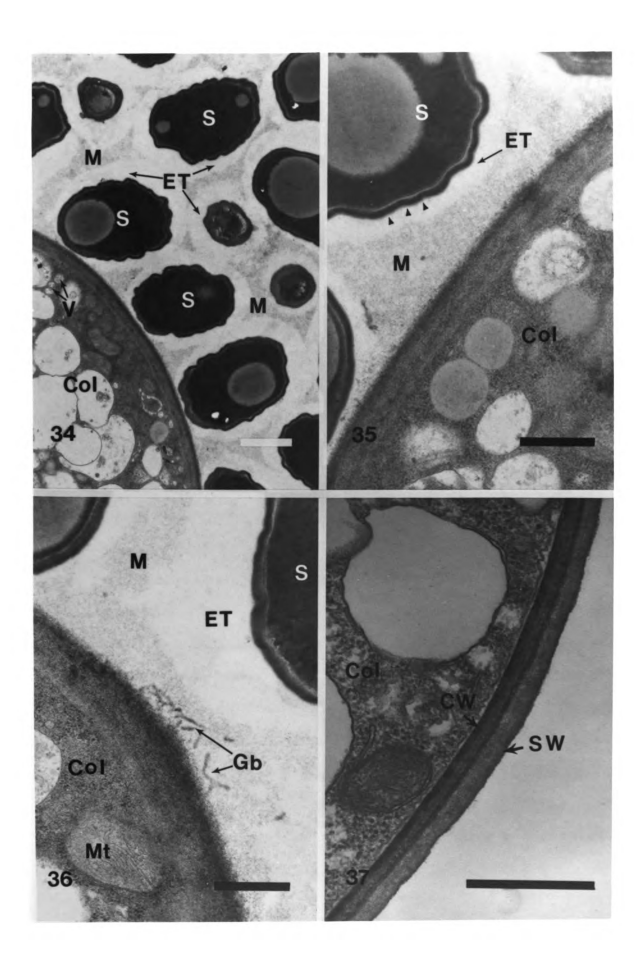
newly formed spore protoplasts outward there was noted: (1) the spore protoplast plasma membrane which was previously defined (Fig. 31) as the cleavage furrow plasma membrane, (2) an 8.0nm electron translucent layer, previously found immediately internal to the plasma membrane in all identifiable cleavage vesicles and furrows, which persisted between the plasma membrane of the spore protoplasts and (3) the electron opaque layer of the spore protoplast, which used to be the granules of the cleavage furrows, (4) an additional 8.0nm electron translucent layer, which had no corresponding layer within the cleavage furrows, (5) a uniform zone of electron transparency, similarly placed in the cleavage furrows, and (6) a non-uniform granular matrix existing between the spore protoplasts (Figs. 31 Maturity of the spore protoplast wall occurred through the condensation of the finely granular particles of the intraspore spaces, (Fig. 31 II, 6), onto the exterior surface of electron opaque layer of the spores, (Fig. 31 II, 3). formed the observable, uniformly electron translucent transitional zone, (Fig. 31 II, 4), and an associated electron transparent zone, which contained concentrations of the intra-spore matrix material, (Fig. 31, 5), (Figs. 28-30, & 34-36).

While the observable matrix of material remained in the spaces between the spores, from early postcleavage through

Figures 32 & 33. Postcleavage. 32. Postcleavage sporangium with mature spines and an furrow (arrows) at the base of the sporangium indicating the internal columella (bar = 10μ m). 33. The base of an unattached postcleavage sporangium, looking up through the sporangiophore (Sph). Note the encircling furrow (arrows) and the lack of spines nearing the junction between the sporangium and the sporangiophore (bar = 5μ m).



Figures 34-36. Mid-postcleavage. 34. The mid-postcleavage sporangium with dense spores (S), a thinning electron translucent matrix between the spores, and a widening electron transparent zone (ET). The columella contains numerous vesicles (V) in its periphery and a vacuolate central region (bar =1 μ m). 35. The electron translucent matrix (M) closely oppressed to the fibrillar columellar wall, and the electron transparent zone (ET) surrounding the spores. Note that the arrow heads indicate the electron translucent outer layer of the spores (bar = $0.5\mu m$). Electron opaque granular bodies (Gb) which appear in the region just outside of the columella (Col) (bar = $0.5\mu m$). 37. A cross section of the very base of the sporangium, exhibiting the ultrastructural differences between the fibrillar columellar wall (CW) and the sporangial wall (SW) $(bar = 0.5\mu m).$



ron

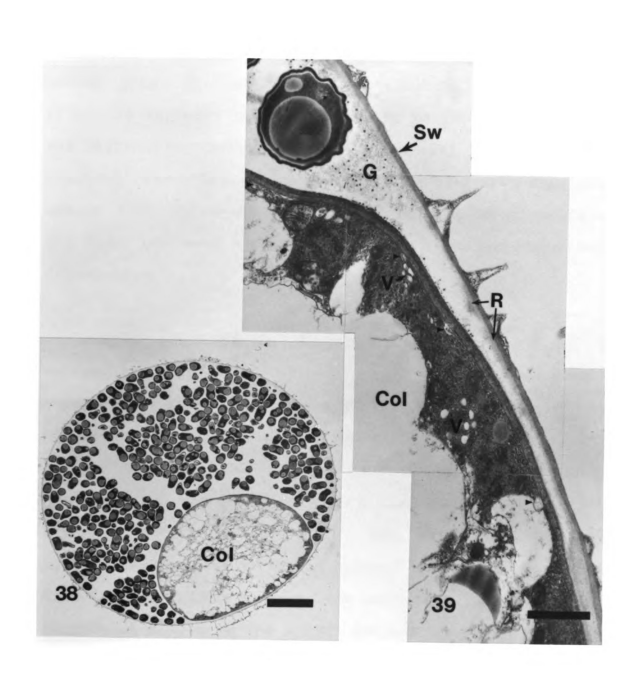
W)

C

mid postcleavage, the spores remained evenly spaced and supported within the matrix of the sporangium (Fig. 34). In mid postcleavage and late postcleavage, after this electron opaque material had coalesced onto the spores they became far more susceptible to being physically moved about within the sporangium interior (Fig. 38). Spores were never observed clumped closely together at any one point within the sporangium. Some material, unstainable and electron transparent in nature, must have remained between the spores providing a supporting matrix which held the spores apart. It was assumed that it was through this electron transparent space between the spores that the enzymes of sporangial wall degradation diffused.

The columellar wall material, as observed since its inception, consisted of a much more fibrillar and electron dense nature, and would most likely be enzymatically distinguishable from that of the sporangial wall itself (Figs. 26, 34, 37-40). In addition, the ultrastructure of the newly-formed walls of the spores was structurally different from the sporangial wall (Figs. 28-43), and remain unaffected by sporangial wall degradative enzymes. Autolysis of the sporangiophore material was observed as numerous vacuoles containing degenerate organelles and crystals distributed in the late-cleavage and postcleavage columellar region. Within the remaining peripheral

Figures 38 & 39. Late postcleavage. 38. Crossection of a late postcleavage sporangium showing how the mature spores were displaced during specimen preparation. Note the lack of electron translucent material between the mature spores (bar = $10\mu m$). 39. Higher magnification of Fig. 38 showing numerous vesicles (V) within the sporangium, arrow heads indicate vesicles fusing with the columellar plasma membrane. Note the electron opaque granules (G) within the sporangial matrix, and the remnants (R) of the secondary wall layer of the sporangial wall (Sw) (bar = $1\mu m$).

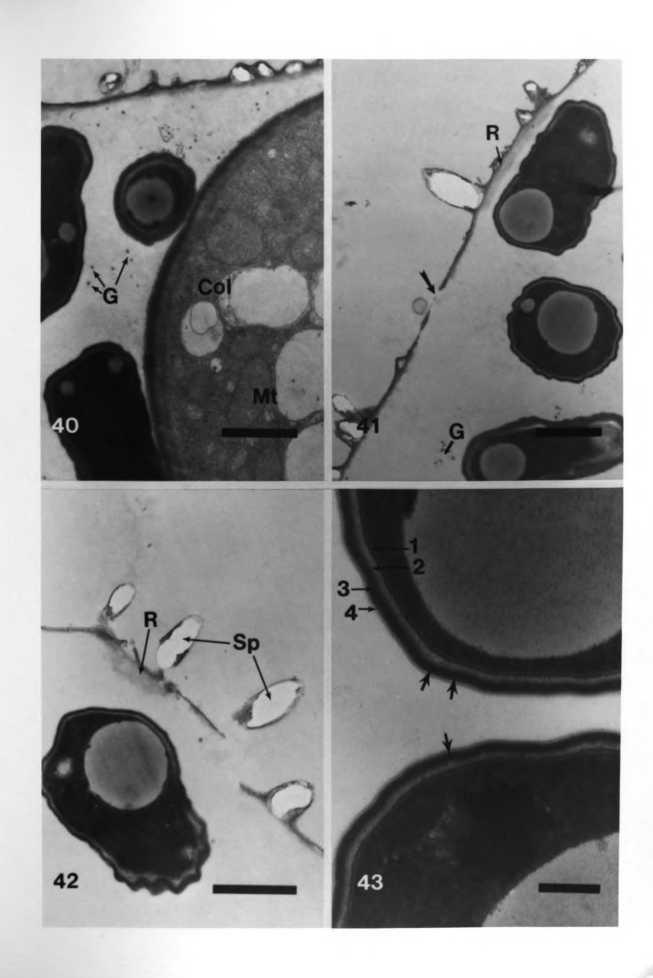


cytoplasm, of the columella, numerous vesicles and endoplasmic reticula, were observed. Many of these vesicles were observed fusing with the columellar plasma membrane (Fig. 39). Numerous electron opaque, granular bodies (Fig. 36) and individual electron opaque granules (Figs. 39-42) were observed exterior to the columellar wall and diffusing throughout the sporangial matrix. These electron opaque granules appeared to be of a very dissimilar nature from those observed within the cleavage apparatus, and were believed to have played role in sporangial wall degradation.

Enzymes appeared to digest accessible areas of the sporangial wall (Figs. 39, 41, 42, 44 & 45). Remnants of secondary sporangial wall material was observed in areas covered by spores closely oppressed to the sporangial wall, (Figs. 39, 41 & 42). Since such internal remnants were observed it was believed that the degradation of the sporangial wall was enzymatic, and since the sporangial plasma membrane was no longer present these enzymes were not membrane bound, but rather were present within the general sporangial matrix in the spaces between the spores.

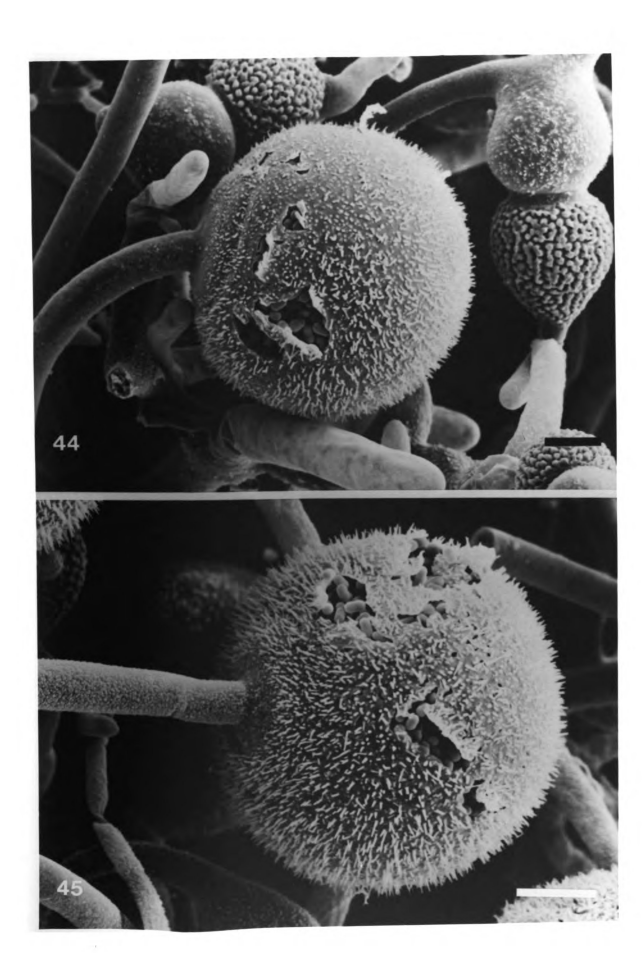
The mature spore walls were composed of four clearly observable layers, the spore plasma membrane (Fig. 43, 1); a secondary spore wall layer (Fig. 43, 2); two outer electron

Figures 40-43. Late postcleavage. 40-42. Mature spores within late postcleavage sporangia, and deliquescence of the sporangial wall (41 & 42). Numerous electron opaque granules (G) are scattered throughout the sporangial matrix (bar = 1μ m). 43. The mature spore wall: (1) the spore plasma membrane, (2) a secondary spore wall layer, (3) two outer electron opaque wall layers, with a denser central interface layer (indicated by the arrows), (4) an electron translucent layer. Note the absence of unstainable material between the spores (bar = 0.2μ m).



Figures 44 & 45. Sporangial wall deliquescence and mature spore release (bar = $10\mu m$).



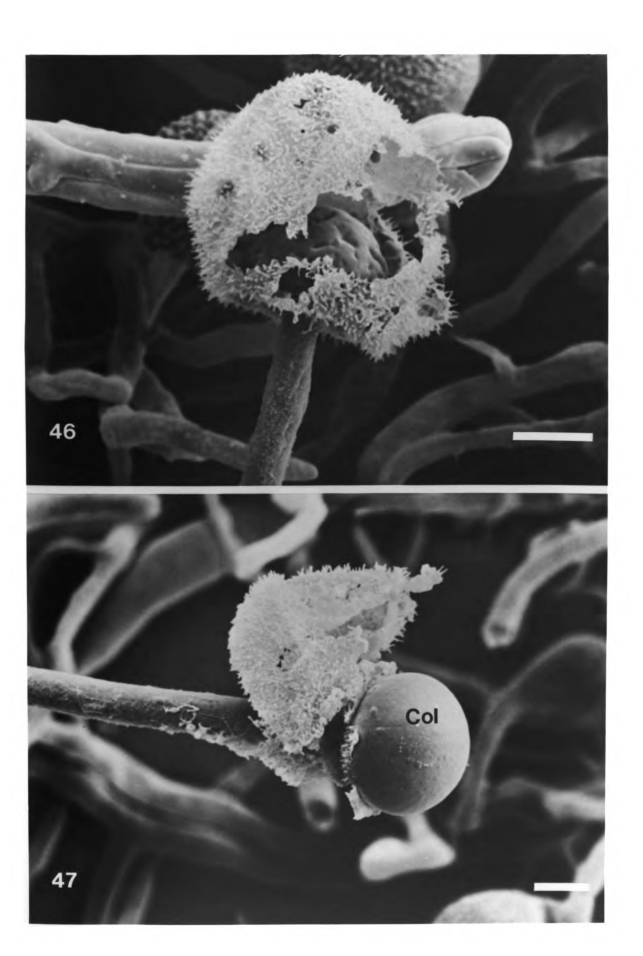


opaque wall layers, with a denser central interface layer (Fig. 43,3); an electron translucent layer (Fig. 43, 4). Mature sporangia measured $43-55\mu m$ in diameter, just prior to spore release. The mature sporangiospores were released through the deliquescence of the sporangial wall (Figs. 46-49). The exposed columellae were found initially fully expanded and smooth, though rapidly became dimpled and collapsed (Fig. 48 & 49).

Additional Observations

During scanning electron microscopic observation Zygorhynchus heterogamus, two notable exceptions to the above detailed descriptions were found. Scattered amongst the normally developing sporangial apparatuses, microsporangial structures were found (Fig. 50). Although uncommon, many repeated observations were made, most often in the areas of peripheral growth of the colonies. micro-sporangiophores measured the typical $8-11\mu m$ diameter, however extended only 0.5-30 µm above the substrate surface. Mature sporangia supported by these microsporangiophores were $23-40\mu m$ in diameter, slightly smaller but very similar to the more typical sporangia, $43-55\mu m$, in diameter. Also noted were rare sporangiophore branchings (Fig. 51). No hyphal structures were observed which bore both sporangia and zygospores.

Figures 46 & 47. Mature sporangiospore release and sporangial wall collapse (bar =10 μ m).



Figures 48 & 49. Complete sporangial degradation, and initiation of columellar collapse (48. bar = $10\mu m$, 49 bar = $5\mu m$).



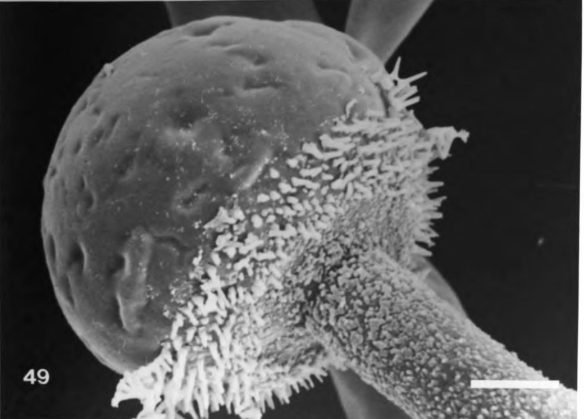
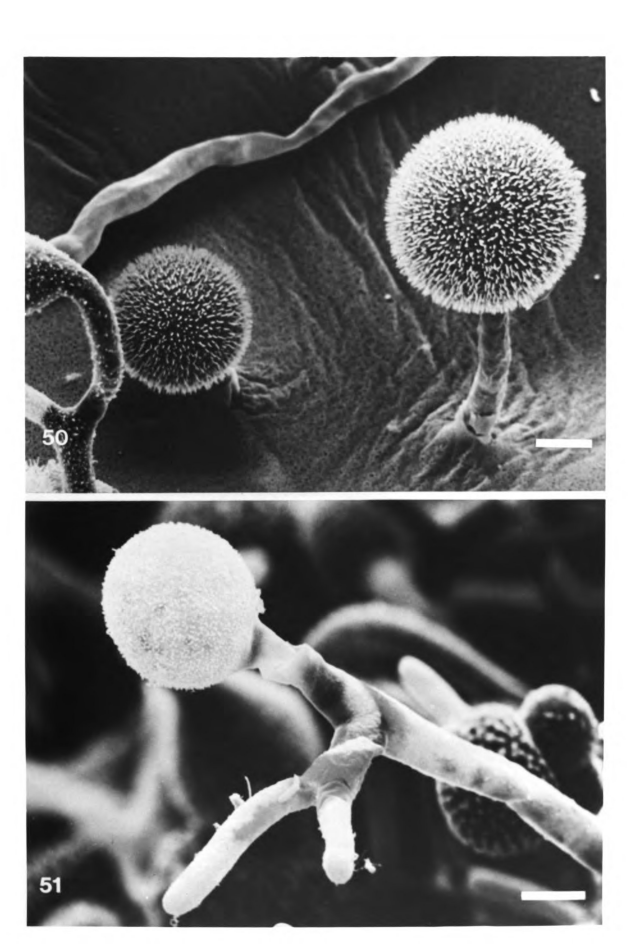


Figure 50. Microsporangia (bar = 10μ m).

Figure 51. A rare branching of a sporangiophore (bar = $10\mu m$).



Discussion

Sporangiosporogenesis is not a series of discrete events but rather a continuum. Sporangiosporogenesis in Zygorhynchus heterogamus can be described as a finely choreographed series of developmental events, but again it must be kept in mind that no single event occurs independently, but rather in conjunction and in interaction with all the others.

It has been reported that the chemical composition of the spines in related members of the Mucorales is primarily calcium oxalate (Jones, et. al., 1976). The X-ray microanalysis of the spines of Z. heterogamus showed a predominance of calcium, and it is believed that these spines are also composed of calcium oxalate. Although it has been proposed that these spines function either in protection or as waste material deposition sites, Hendler and Hammill (1986) reported that these spines were lacking in aborted sporangia of Mucor mucedo, and perhaps played some more crucial role in sporangiosporogenesis, though the exact nature of this role remains to be defined.

Bartnicki-Garcia (1968) reported that the sporangial walls of members of the Mucorales closely related to \underline{Z} .

heterogamus, were of a completely different nature than their spores, chitin/chitosan versus melanin impregnated glucan, respectively. Further he observed that it was only in the sporangiospores of these fungi that glucans were found (Bartnicki-Garcia, 1968). This is believed to also be true of Z. heterogamus, accounting for the observable differences between the electron dense spore walls and the electron translucent, layered sporangial wall. Such a chemical difference would support the concept that the enzymes responsible for sporangial wall degradation could be released into the general sporangial matrix, and yet, specifically target the sporangial wall.

Autolysis of the sporangiophore material was observed in Z. heterogamus as numerous vacuoles containing degenerate organelles and crystals distributed in the late-cleavage and postcleavage columellar region. Within the remaining peripheral cytoplasm, of the columella, numerous vesicles and endoplasmic reticula, were observed as well as vesicles which fused with the columellar plasma membrane. It can be proposed that through the catabolic turnover of the sporangiophoric materials within the columellar region, sporangial wall degradative enzymes are synthesized, transported through the fibrillar columellar wall, and released into the sporangial matrix. Diffusing through the electron opaque matrix of the sporangium these enzymes

appeared to digest readily accessible areas of the sporangial wall, resulting in sporangial deliquescence and spore release.

If the thickening of the mature spore walls, as observed in Gilbertella persicaria (Bracker 1966,1968) and Mucor mucedo (Hammill 1981) and not in Z. heterogamus are not due to species differences but are artifacts of preparation, as indicated by light microscopy, then an explanation for this discrepancy needs to be found. The electron transparent internal thickening of the spore wall as observed by Hammill (1981) in his micrographs of in the mature spores of M. mucedo may be more correctly interpreted as an artifact in preparation caused by osmotic collapse. This electron transparent region lacks any detail and the plasma membrane contour of the spores perfectly matches the spore wall contour, both of which are common features of osmotic collapse. Additionally, his specimen preparation technique did not include an osmotic buffer, my observations of Z. heterogamus found it to be very susceptible to osmotic pressures.

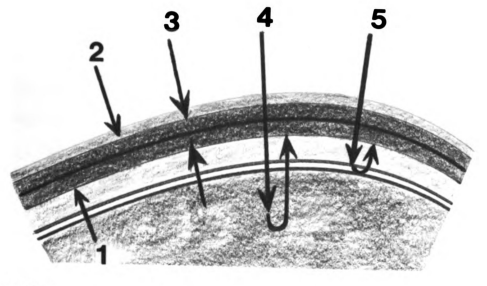
This same electron translucent, secondary thickening of mature spore walls as observed by Bracker (1968) with its extremely indistinct structure should also be suspect of osmotic collapse. Bracker's use of potassium permanganate,

KMnO₄, which is currently viewed as resulting in poor ultrastructural preservation when compared to other techniques, might explain the lack of ultrastructural detail, and explain his interpretation of a second internal spore wall. These discrepancies of wall structure could be sorted out utilizing the techniques of low-voltage, high resolution SEM of fractured spores or through the use TEM observation of freeze fracture replicas of fractured spores.

Five methods of spore wall deposition can be proposed which incorporate the ultrastructural observations made of Z. heterogamus (Fig. 52). First, as was proposed and supported by Bracker (1966, 1968), and Hammill (1981) all but the very outer layer of the spore wall are synthesized and laid down by the spore cytoplasm (Fig. 52, 1). This however, does not account for the progressive loss of the granular matrix material found between the spores. Second, the entire spore wall is laid down exogenously, from what was once the cleavage furrow matrix (Fig. 52, 2), however this would seem unlikely, due to the apparent complexities of fungal wall synthesis. However, there has been no report specifically detailing spore wall synthesis or glucan synthesis in the Mucorales.

Due to the method of $KMnO_4$ fixation utilized by Bracker (1966,1968), he failed to notice the significance of the

Figure 52. Zygorhynchus heterogamus. An illustrative diagram of five proposed methods of spore wall formation. (1) The endogenous deposition of spore wall material. (2) the exogenous deposition of spore wall material via a "condensation" of the electron translucent material found within the matrix between the postcleavage spores. (3) A combination of endogenous and exogenous deposition of (4) The transport of the electron translucent material. matrix material into the spore interior for conversion into spore wall material and endogenous deposition. (5) The transport of the electron translucent material through the wall layers to the spore plasma membrane where enzyme complexes of the plasma membrane convert it into spore wall material.



just after post cleavage. This is the layer which was previously defined as an electron translucent layer of transition of Z. heterogamus. It is this layer which may mark an exogenous deposition of spore wall material, rather than endogenous as previously proposed for G. persicaria and M. mucedo.

Bartnicki-Garcia found that the spore walls of fungi closely related to Z. heterogamus lacked the layered ultrastructure readily observed within the vegetative hyphal walls, but rather exhibited a highly, densely organized uniform structure (personal communication). structure of the spore wall can be viewed as a crystalline matrix of branched R-glucan molecules, this would explain the observed 'condensation' of material from the matrix between the spores onto the spore walls. Walls constructed in such a fashion would not need major enzyme complexes, nor substantial energy input, but rather would be a fairly simple synthesis allowing for an exogenous deposition of wall material. However this does not explain the observed deposition of material, of an ultrastructurally observably different nature than the electron opaque spore wall layer, between the electron opaque layer and the spore plasma membrane.

Accounting for this layer indicates a third possible proposal of spore wall synthesis, that the wall is laid down from both the interior and exterior (Fig. 52, 3). The exterior deposition forming the electron opaque outer layer of the wall via a 'condensation' of the matrix material between the spores, and the interior deposition of the secondary inner wall layer. However, this method still requires dense organization of the outer spore wall layers theoretically without major enzyme complexes or energy input, because it is extracellular.

This brings forth the proposal of a fourth and fifth method of spore wall synthesis. Accounting for the progressive loss of the granular matrix material found between the spores, this material may pass through the outer electron opaque layer of the spore and be utilized as a fundamental component of the spore wall metabolized within the matrix of the spore itself (Fig. 52, 4), and be endogenously deposited. Finally perhaps rather than passing into the spore itself, the matrix material may be synthesized into wall components, by enzyme complexes situated on and/or within the plasma membrane of spore, and there be deposited.

In general it was found that, with the few exceptions listed above, sporangiospore development in Zygorhynchus

heterogamus occurred in the same fashion as that described for Gilbertella persicaria, by Bracker (1966, 1968), and Mucor mucedo, by Hammill (1981). The Brackerian model for sporangiosporogensis should be considered to hold true for multispored sporangiosporogenesis within the Mucorales. Although, the ultrastructural events, in Z. heterogamus, resulting in the maturation of the spore walls may be found to be more of a combined exogenous and endogenous process.

LIST OF REFERENCES

- Bartnicki-Garcia, S. 1968. Cell wall chemistry, morphogenesis, and taxonomy of fungi. Annual Review of Microbiology 22: 87-108.
- Benjamin, R.K. 1979. Zygomycetes and their spores. In <u>The Whole Fungus</u> (Ed. B. Kendrick). Vol. 2, pp. 573-616. National Museum of Natural Sciences, National Museums of Canada, Ottawa.
- Bracker, C.E. 1966. Ultrastructural aspects of sporangiospore formation in <u>Gilbertella persicaria</u>. In <u>The Fungus Spore</u> (Ed. M.F. Madelin). pp. 39-60. Butterworths (London, England).
- Bracker, C.E. 1968. The ultrastructure and development of sporangia in <u>Gilbertella persicaria</u>. Mycologia 60: 1016-1067.
- Cole, G.T. and Samson, R.A. 1979. <u>Patterns of Development in Conidial Fungi</u>. Pitman Publishing Ltd. (London, England).
- Domsch, K.H., Gams, W., and Traute-Heidi Anderson. 1980.

 <u>Compendium of Soil Fungi</u>. Academic Press (London, England).
- Hammill, T.M. 1981. Mucoralean sporangiosporogenesis. In <u>The Fungal Spore: Morphogenetic Controls</u> (Ed. H.R. Hohl). pp. 173-194. Academic Press (New York).
- Hammill, T.M., and Secor, D.L. 1983. The number of nuclei in sporangiospores of <u>Mucor mucedo</u>. Mycologia 75: 311-315.
- Hanlin, R. T., translator. 1973. Keys to the families.

 genera and species of the Mucorales. Verlag von J.

 Cramer (Leutershausen, Germany). Orginally published
 in Mucorales by H. Zycha and R. Siepmann, 1969, Verlag
 von J. Cramer (Lehre, Germany)

- Hendler, J. and Hamill, T.M. 1986. The influence of KMnO₄ on sporangial development in <u>Mucor mucedo</u>. Poster presentation at the annual Mycological Society of America's 1986 meeting, Amherst, Mass.
- Hesseltine, C.W., Benjamin, C.R., and Mehrotra, B.S. 1959. The genus Zygorhynchus. Mycologia 51:173-194.
- Hesseltine, C.W., and Ellis, J.J. 1973. Mucorales. In: The Fungi. An advanced treatise, Vol. IV B. A Taxonomic Review With Keys: Basidomycetes and Lower Fungi. (Eds. G.C. Ainsworth, F.K. Sparrow, and A.S. Sussman.) Academic press (New York).
- Jones, D., McHardy, W.J. and Wilson, J.J. (1976). Ultrastructure and chemical composition of spines in Mucorales. Transactions of the British Mycological Society. 65: 153-157.